



Published in final edited form as:

Biochem Biophys Res Commun. 2015 April 10; 459(3): 463–468. doi:10.1016/j.bbrc.2015.02.128.

Chloride concentrations in human hepatic cytosol and mitochondria are a function of age

Stephan C. Jahn¹, Laura Rowland-Faux¹, Peter W. Stacpoole^{2,3}, and Margaret O. James^{1,*}

¹Department of Medicinal Chemistry, University of Florida, Gainesville, FL 32610-0485, United States

²Department of Medicine, University of Florida, Gainesville, FL 32610-0226, United States

³Department of Biochemistry and Molecular Biology, University of Florida, Gainesville, FL 32610, United States

Abstract

We recently reported that, in a concentration-dependent manner, chloride protects hepatic glutathione transferase zeta 1 from inactivation by dichloroacetate, an investigational drug used in treating various acquired and congenital metabolic diseases. Despite the importance of chloride ions in normal physiology, and decades of study of chloride transport across membranes, the literature lacks information on chloride concentrations in animal tissues other than blood. In this study we measured chloride concentrations in human liver samples from male and female donors aged 1 day to 84 years (n = 97). Because glutathione transferase zeta 1 is present in cytosol and, to a lesser extent, in mitochondria, we measured chloride in these fractions by high-performance liquid chromatography analysis following conversion of the free chloride to pentafluorobenzylchloride. We found that chloride concentration decreased with age in hepatic cytosol but increased in liver mitochondria. In addition, chloride concentrations in cytosol, (105.2 ± 62.4 mM; range: 24.7 – 365.7 mM) were strikingly higher than those in mitochondria (4.2 ± 3.8 mM; range 0.9 – 22.2 mM). These results suggest a possible explanation for clinical observations seen in patients treated with dichloroacetate, whereby children metabolize the drug more rapidly than adults following repeated doses, and also provide information that may influence our understanding of normal liver physiology.

Keywords

chloride; liver; cytosol; mitochondria; dichloroacetate; GSTZ1

© 2015 Published by Elsevier Inc.

*Corresponding author: Department of Medicinal Chemistry, PO Box 100485, University of Florida, Gainesville, FL 32610-0485, Tel.: +1 352 273 7707, fax: +1 352 846 1972, mojames@ufl.edu.

Publisher's Disclaimer: This is a PDF file of an unedited manuscript that has been accepted for publication. As a service to our customers we are providing this early version of the manuscript. The manuscript will undergo copyediting, typesetting, and review of the resulting proof before it is published in its final citable form. Please note that during the production process errors may be discovered which could affect the content, and all legal disclaimers that apply to the journal pertain.

Introduction

The chloride ion is an essential electrolyte and is the predominant anion in extracellular fluid. It functions importantly in many fundamental biological processes, including regulation of pH, maintenance of intracellular volume and resting membrane potential and cell growth and differentiation [1,2]. Transport of chloride across cell membranes is facilitated by both voltage-gated and non-voltage-gated chloride channels [3]. Hyperchloremic metabolic acidosis, myocardial dysfunction, renal tubular defects and cystic fibrosis are among the many pathological conditions associated with disruption of chloride homeostasis [1,3,4].

The extensive literature on chloride physiology and pathophysiology is restricted mainly to assessing changes in extracellular fluid chloride levels or ion flux and largely neglects measurements of intracellular compartmental chloride concentrations. We recently reported that in a concentration-dependent manner, chloride and certain other anions protect glutathione transferase zeta 1 (GSTZ1) from irreversible inactivation by DCA [5]. DCA is a mechanism-based inhibitor of GSTZ1, reportedly by adduct formation with the protein [6]. GSTZ1 also functions as maleylacetoacetate isomerase, the penultimate enzyme in the catabolism of tyrosine. Inhibition of this isomerization step by DCA leads to accumulation of reactive tyrosine and heme intermediates that have been implicated in a reversible peripheral neuropathy associated with chronic DCA exposure [7]. This is of interest because DCA is an investigational drug used to treat acquired and inborn errors of mitochondrial bioenergetics [7], and is converted to an inactive metabolite, glyoxylate by GSTZ1 [8]. Thus, factors that influence the interaction of DCA and GSTZ1 have significant clinical import.

Differences in DCA pharmacokinetics, likely due to rates of inactivation of GSTZ1, exist in patients of varying age, with older patients exhibiting pharmacokinetic evidence of a greater extent of inactivation and increased incidence of side effects [9]. A possible explanation for these observations is a decrease in liver cytosolic chloride concentration ($[Cl^-]$) as age increases, which would lead to more rapid GSTZ1 inactivation. While the $[Cl^-]$ in serum is well characterized, ranging from 98–106 mM [10], we found only one report of $[Cl^-]$ in human liver. The 1960 paper by Widdowson and Dickerson found liver $[Cl^-]$ to be 55.8 mM in newborns, 42.8 mM in 4–7 month olds, and 38.3 mM in adults [11]. These groups were comprised of 4, 3, and 4 individuals, respectively, and the ages of the adults were not given. The reported concentrations were for whole-liver lysates and therefore do not represent any cellular environment in which GSTZ1 exists. Two additional studies reported the intracellular $[Cl^-]$ in cultured rat hepatocytes to be 38 mM [12] and 30.1 mM [13], respectively.

In the current study we characterized the $[Cl^-]$ in liver over a wide age range of donors. We determined chloride concentration in both cytosolic and mitochondrial compartments, as well as in whole liver for a sub-set of the samples. Standard gravimetric determination of chloride is very laborious and chloride-selective ion probes suffer from interference due to bile salts [14], making them impractical to use on liver samples. The HPLC method we employed allows rapid, accurate and highly reproducible results. Our findings show that

there are major changes in cellular $[Cl^-]$ that occur during human development, providing valuable information that can be used to better predict patient response to DCA.

Materials and Methods

Materials and liver samples

All reagents were purchased from Sigma Aldrich (St. Louis, MO) and were the highest purity available, unless otherwise specified. Normal human liver samples were obtained from the Cooperative Human Tissue Network, University of Alabama at Birmingham, the NICHD Brain and Tissue Bank of the University of Maryland and the University of Florida Clinical and Translational Science Institute.

Chloride Derivatization and Chromatography

The method used was based on that described by Tsikas et al. [15], with minor modifications to facilitate use with more complex biological samples and to improve chromatographic separation. The process involves conversion of pentafluorobenzyl bromide to pentafluorobenzyl chloride when the bromide form is added to a sample containing chloride (Figure 1A). Acetone (400 μ L) was added to 50 μ L of cytosol or mitochondria sample, prepared as previously described [16], or to 50 μ L of sonicated whole liver homogenate in water. Mitochondrial samples were lysed by sonication. After vortexing, the mixture was incubated at -20 $^{\circ}C$ for 1 hour prior to centrifuging at 16,000 g at 4 $^{\circ}C$ to pellet insoluble components. The supernatant was transferred to a clean tube and 10 μ L of 2,3,4,5,6-pentafluorobenzyl bromide was added in a fume hood. The solution was mixed and incubated in a capped tube at 50 $^{\circ}C$ for 30 minutes. Acetone was removed under a gentle stream of nitrogen gas and the remaining aqueous solution was mixed with 400 μ L of 75/25 acetonitrile/water containing 25 μ M *p*-hydroxybiphenyl, which served as the internal standard. The resulting solution was passed through a 0.45 or 0.22 μ m nylon spin filter (Costar, Tewksbury, MA) before loading 50 μ L onto a Discovery C-18 column (Sigma Aldrich) attached to either a Shimadzu CBM-20A (Kyoto, Japan) or Beckman-Coulter System Gold (Brea, CA) HPLC instrument and eluted using a 1:1 acetonitrile:water mobile phase at 1 mL/minute. UV absorbance of the eluent was monitored at 264 nm.

Construction of Standard Curves and calculation of $[Cl^-]$

Standard curves were generated by injecting a series of samples consisting of the buffer used for that subcellular fraction [16] that contained increasing concentrations of NaCl that appropriately represented the $[Cl^-]$ range in the cytosol (0.5 to 7.5 mM) or mitochondria (0.01 to 1 mM), and a fixed concentration, 25 μ M, of 4-hydroxybiphenyl as internal standard. For the whole liver homogenate samples, the standard curve was prepared in water and concentrations ranged from 5 to 20 mM. Areas for the pentafluorobenzyl chloride peak were normalized by taking the ratio of this peak to the internal standard peak. Plots of the peak ratio against the concentration of $[Cl^-]$ were linear and the slope and intercept values were used to calculate the $[Cl^-]$ in samples. The raw $[Cl^-]$ was corrected for the dilution of the sample (using a liver density of 1 g/mL). This value was then converted to either a cytosolic or mitochondrial $[Cl^-]$ by dividing by constant factors of 0.364 or 0.148,

respectively, as the liver is reported to be composed of 36.4% cytosol and 14.8% mitochondria [17].

Results

Assay parameters and validation

The HPLC conditions gave excellent separation of the pentafluorobenzyl chloride peak (19.5 min) from the internal standard (9 min) and from pentafluorobenzyl bromide (22 min). Studies with dialyzed liver cytosol and mitochondria to which no chloride was added showed that there were no interfering peaks at the retention time of pentafluorobenzyl chloride. Addition of a known concentration of chloride to dialyzed liver cytosol or mitochondria gave a peak at 19.5 min. Figure 1B shows a representative chromatogram from liver cytosol. The ratio of the pentafluorobenzyl chloride peak area to the internal standard peak area was linear with increasing $[\text{Cl}^-]$ up to at least 20 mM. Replicate standard curves prepared on different days showed that inter-day variability was less than 10%. Although different buffers or water were used to prepare standard curves for mitochondria, cytosol and whole liver, there was no evidence of a buffer effect (Table 1). The limit of detection, calculated as the concentration that gave a signal to noise ratio of at least 3, was 0.05 mM, and the limit of quantitation was 0.1 mM. Table 1 shows parameters for the standard curves used for mitochondria, cytosol and whole liver.

Recovery studies were carried out by spiking a mitochondrial sample with additional chloride. This yielded concentrations that were calculated to be the sum of the endogenous and added anion. Addition of 0.25 mM chloride resulted in recovery of $101.9 \pm 5.1\%$ of the added chloride and addition of 1 mM resulted in recovery of $94.7 \pm 4.0\%$ of the added chloride.

Measurement of $[\text{Cl}^-]$ in whole human liver homogenates

In order to provide a point of reference for which to compare our cytosolic and mitochondrial samples, we determined the $[\text{Cl}^-]$ in a subset of 32 whole liver homogenate samples that appropriately represented the range of ages in our complete dataset. After accounting for sample dilution, the calculated concentrations represent the mean $[\text{Cl}^-]$ in each liver sample. We obtained a range of 25.1 to 62.9 mM Cl^- and a mean of 42.0 ± 9.0 mM Cl^- (Figure 2A). A Spearman correlation showed that there was not a relationship between whole liver $[\text{Cl}^-]$ and age ($p > 0.1$). There was a statistically significant increase of the ratio of whole liver chloride to cytosolic chloride (cytosolic data from Figure 3) with increasing age (Figure 2B, slope = 0.557, $p < 0.001$).

Determination of human liver cytosolic and mitochondrial $[\text{Cl}^-]$

Liver samples from 97 donors, ranging in age from 1 day to 84 years, were separated into cytosolic and mitochondrial fractions as described previously [16]. The cytosolic $[\text{Cl}^-]$, corrected for the volume of cytosol in liver, had a minimum of 29.7 mM, a maximum of 365.7 mM, and a mean of 105.2 ± 62.4 mM. Plotting cytosolic $[\text{Cl}^-]$ against donor age (Figure 3A) shows a striking change with increasing age that becomes even more pronounced when age is plotted on a logarithmic scale (Figure 3B). As donor age increases,

both the average cytosolic $[Cl^-]$ and the variability between donors decreases. The Spearman correlation between these two parameters yields an r value of -0.552 with a two-tailed $p < 0.0001$. A node is visible in the data around the age of 10,000 days, which is approximately 27 years of age. Donors below this cutoff had a mean cytosolic $[Cl^-]$ of 125.2 mM while those above this age had a mean of 75.4 mM Cl^- (Figure 3C).

The mitochondrial $[Cl^-]$, corrected for the volume of mitochondria in liver, ranged from 0.9 mM to 22.2 mM (mean = 4.2 ± 3.8 mM) and was weakly correlated with age ($r = 0.247$; $p < 0.05$). However, the absolute values changed only slightly and are much lower than the cytosolic concentrations. This trend can be seen with age plotted on a linear (Figure 4A) or logarithmic (Figure 4B) scale. The mitochondrial $[Cl^-]$ shows a highly significant difference compared to the cytosolic concentration (Figure 4C). Our data showed there was an inverse trend ($r = -0.189$, $p < 0.1$) between mitochondrial and cytosolic $[Cl^-]$ (Figure 4D) in individual donors, although this is likely due to their mutual correlation with age, rather than to a cause and effect relationship in the two compartments. There was no discernable difference in $[Cl^-]$ when analyzed according to gender or race (data not shown). The raw data for cytosolic, mitochondrial, and whole liver chloride concentrations are provided in Supplementary Table 1.

Discussion

Using an HPLC-based method for determining $[Cl^-]$ in biological tissues, we have measured the $[Cl^-]$ in whole human liver as well as in the cytosolic and mitochondrial compartments. Our whole liver concentrations closely matched the limited data that have previously been published [11]. While this confirms the previous work and validates the method we used, this concentration has little relevance to our study of DCA metabolism by GSTZ1, because the enzyme is not found at any subcellular compartment exhibiting that $[Cl^-]$.

In the cytosol, there was a striking decrease of $[Cl^-]$ as donor age increased. Interestingly, this correlates with changes in the pharmacokinetics and side effects that have been observed in patients treated with DCA [9]. In those studies, adult subjects exhibited decreased rates of clearance and increased side effects after repeated doses of DCA. Young patients were less likely to show these phenomena and they are thought to be related to differences in the rate of GSTZ1 inactivation, although the cause of that difference was unknown [18,19]. The current data, along with those we have recently published showing a protective effect of chloride on the rate of inactivation of GSTZ1 during DCA metabolism [5], make it likely that the increased cytosolic chloride concentration in the livers of young patients, where the majority of GSTZ1 is located, decreases their rates of GSTZ1 inactivation.

Interestingly, the cytosolic $[Cl^-]$ was much higher than that found in the whole liver homogenate. This hints that the remainder of the liver (organelles, extracellular matrix, etc.) has very low chloride content. However, age is not associated with a change in whole liver $[Cl^-]$ but is inversely associated with cytosolic $[Cl^-]$, which leads to an increase in the ratio of the whole liver $[Cl^-]$ to cytosolic $[Cl^-]$. One possible explanation for this observation is that $[Cl^-]$ increases in one or more compartments while decreasing in the cytosol. It is

unclear what this other compartment may be (extracellular matrix, nuclei, endoplasmic reticulum, etc.). Future studies are required to resolve this uncertainty.

The mitochondria are both the major site of DCA dynamics [7] and a significant site of biotransformation [16]. In contrast to our findings in liver cytosol, we observed a noticeable increase in mitochondrial $[Cl^-]$ with age, although it was not as dramatic as was the age-related decline in cytosolic $[Cl^-]$. Regardless of the magnitude of this increase, the major observation is that the cytosolic $[Cl^-]$ was often over 10x higher than the mitochondrial $[Cl^-]$. This finding suggests that DCA-induced inactivation of GSTZ1 may occur more rapidly in mitochondria than in cytoplasm. Animal studies to test this postulate are currently underway. However, when viewed through the lens of a whole animal, rapid inactivation of mitochondrial GSTZ1 may not have a major consequential impact on DCA metabolism or toxicity, because 86% of liver GSTZ1 is located in the cytosol [16].

There was an inverse correlation between cytosolic and mitochondrial $[Cl^-]$ in liver from the same donor. Therefore, the mechanism resulting in increased cytosolic $[Cl^-]$ is likely independent of that regulating mitochondrial $[Cl^-]$. The plasma membrane contains multiple types of chloride channels that are activated by swelling [20] or Ca^{2+} [21]. Conversely, the mitochondria contain only voltage-gated anion channels [22]. Because mitochondrial function is strongly dependent on ion gradients, it would be expected that these gradients would be well regulated and not vary greatly with age, to keep the $[Cl^-]$ near optimal. This possibly explains the minor change in mitochondrial chloride levels in terms of absolute values.

A potential limitation of this work is our reliance on cytosolic and mitochondrial volume in rat hepatocytes [15], because similar data in humans is not available. Nevertheless, our results represent the first large-scale developmental study to examine chloride concentrations in the human liver. As chloride concentrations impact GSTZ1 stability and therefore DCA kinetics, the data presented here could be used to help determine proper patient dosing. They not only provide valuable information that will be used in the treatment of patients with DCA, but also raise questions regarding the normal physiology of chloride in cells. It is our hope that others will find additional uses for these data as well.

Supplementary Material

Refer to Web version on PubMed Central for supplementary material.

Acknowledgments

We thank Dr. Pippa Simpson at the Medical College of Wisconsin for her help in analyzing the data as well as Marci Smeltz and Guo Zhong at the University of Florida for their help in preparing the tissue fractions and Ryan Lorenzo for his help with the HPLC analyses. This work was funded by a grant from the US Public Health Service, 1 RO1 GM 099871, by an NCI grant to the Cooperative Human Tissue Network and an NIH Contract to the University of Maryland Brain and Tissue bank, HHSN 271 201 4000 45C and by the NIH/NCATS Clinical and Translational Science award to the University of Florida UL1 TR000064.

Abbreviations

GSTZ1	glutathione transferase Z1
DCA	dichloroacetate
Cl⁻	chloride concentration

References

1. Yunos NM, Bellomo R, Story D, Kellum J. Bench-to-bedside review: Chloride in critical illness. *Crit Care*. 2010; 14:226. [PubMed: 20663180]
2. Lang F, Shumilina E, Ritter M, Gulbins E, Vereninov A, Huber SM. Ion channels and cell volume in regulation of cell proliferation and apoptotic cell death. *Contrib Nephrol*. 2006; 152:142–160. [PubMed: 17065810]
3. Jentsch TJ, Stein V, Weinreich F, Zdebik AA. Molecular structure and physiological function of chloride channels. *Physiol Rev*. 2002; 82:503–568. [PubMed: 11917096]
4. Hiraoka M, Kawano S, Hirano Y, Furukawa T. Role of cardiac chloride currents in changes in action potential characteristics and arrhythmias. *Cardiovasc Res*. 1998; 40:23–33. [PubMed: 9876314]
5. Zhong G, Li W, Gu Y, Langaee T, Stacpoole PW, James MO. Chloride and other anions inhibit dichloroacetate-induced inactivation of human liver GSTZ1 in a haplotype-dependent manner. *Chem Biol Interact*. 2014; 215C:33–39. [PubMed: 24632415]
6. Anderson WB, Liebler DC, Board PG, Anders MW. Mass spectral characterization of dichloroacetic acid-modified human glutathione transferase zeta. *Chem Res Toxicol*. 2002; 15:1387–1397. [PubMed: 12437329]
7. Stacpoole PW. The dichloroacetate dilemma: environmental hazard versus therapeutic goldmine--both or neither? *Environ Health Perspect*. 2011; 119:155–158. [PubMed: 20920954]
8. James MO, Cornett R, Yan Z, Henderson GN, Stacpoole PW. Glutathione-dependent conversion to glyoxylate, a major pathway of dichloroacetate biotransformation in hepatic cytosol from humans and rats, is reduced in dichloroacetate-treated rats. *Drug Metab Dispos*. 1997; 25:1223–1227. [PubMed: 9351896]
9. Shroads AL, Guo X, Dixit V, Liu HP, James MO, Stacpoole PW. Age-dependent kinetics and metabolism of dichloroacetate: possible relevance to toxicity. *J Pharmacol Exp Ther*. 2008; 324:1163–1171. [PubMed: 18096758]
10. The Merck Manual of Diagnosis and Therapy. *Clinical and Experimental Optometry* (18). 2007; 90:64–64.
11. Widdowson EM, Dickerson JW. The effect of growth and function on the chemical composition of soft tissues. *Biochem J*. 1960; 77:30–43. [PubMed: 13785015]
12. Bear CE, Petrunka CN, Strasberg SM. Evidence for a channel for the electrogenic transport of chloride ion in the rat hepatocyte. *Hepatology*. 1985; 5:383–391. [PubMed: 2581880]
13. Scharshmidt BF, Stephens JE. Transport of sodium, chloride, and taurocholate by cultured rat hepatocytes. *Proc Natl Acad Sci U S A*. 1981; 78:986–990. [PubMed: 6940160]
14. Lyall V, Croxton TL, Armstrong WM. Measurement of intracellular chloride activity in mouse liver slices with microelectrodes. *Biochim Biophys Acta*. 1987; 903:56–67. [PubMed: 3651457]
15. Tsikas D, Fauler J, Frölich JC. Determination of chloride in biological fluids as pentafluorobenzylchloride by reversed-phase high-performance liquid chromatography and UV detection. *Chromatographia*. 1992; 33:317–320.
16. Li W, James MO, McKenzie SC, Calcutt NA, Liu C, Stacpoole PW. Mitochondrion as a novel site of dichloroacetate biotransformation by glutathione transferase zeta 1. *J Pharmacol Exp Ther*. 2011; 336:87–94. [PubMed: 20884751]
17. Sokirchenko IA, Shkurupii VA. Time course of changes in rat hepatocyte ultrastructure after hepatic ischemia. *Bulletin of Experimental Biology and Medicine*. 1985; 100:1273–1276.

18. Stacpoole PW, Kerr DS, Barnes C, Bunch ST, Carney PR, Fennell EM, Felitsyn NM, Gilmore RL, Greer M, Henderson GN, Hutson AD, Neiberger RE, O'Brien RG, Perkins LA, Quisling RG, Shroads AL, Shuster JJ, Silverstein JH, Theriaque DW, Valenstein E. Controlled clinical trial of dichloroacetate for treatment of congenital lactic acidosis in children. *Pediatrics*. 2006; 117:1519–1531. [PubMed: 16651305]
19. Shroads AL, Coats BS, McDonough CW, Langae T, Stacpoole PW. Haplotype variations in glutathione transferase zeta 1 influence the kinetics and dynamics of chronic dichloroacetate in children. *J Clin Pharmacol*. 2015; 55:50–55. [PubMed: 25079374]
20. Meng XJ, Weinman SA. cAMP- and swelling-activated chloride conductance in rat hepatocytes. *Am J Physiol*. 1996; 271:C112–120. [PubMed: 8760036]
21. Koumi S, Sato R, Aramaki T. Characterization of the calcium-activated chloride channel in isolated guinea-pig hepatocytes. *J Gen Physiol*. 1994; 104:357–373. [PubMed: 7807053]
22. Roos N, Benz R, Brdiczka D. Identification and characterization of the pore-forming protein in the outer membrane of rat liver mitochondria. *Biochim Biophys Acta*. 1982; 686:204–214. [PubMed: 7082663]

Highlights

- This study is the first large scale measurement of hepatic chloride in any species.
- The chloride concentration is much higher in human hepatic cytosol than in the mitochondria.
- Chloride concentration decreases with age in the cytosol while increasing in the mitochondria.

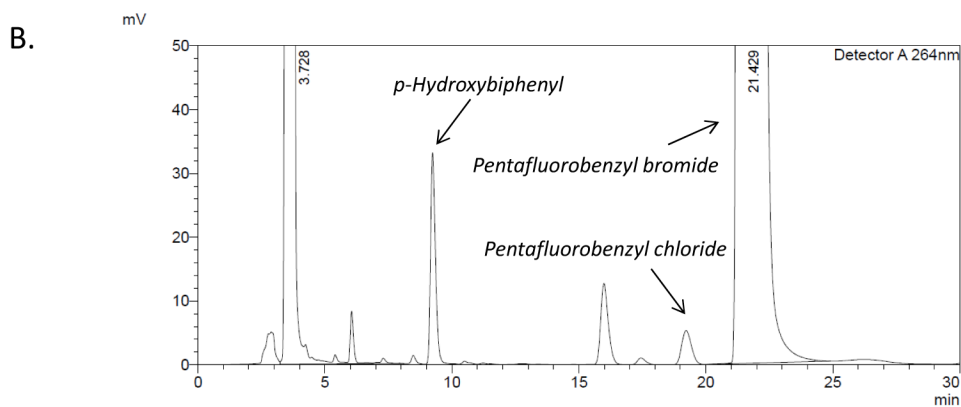
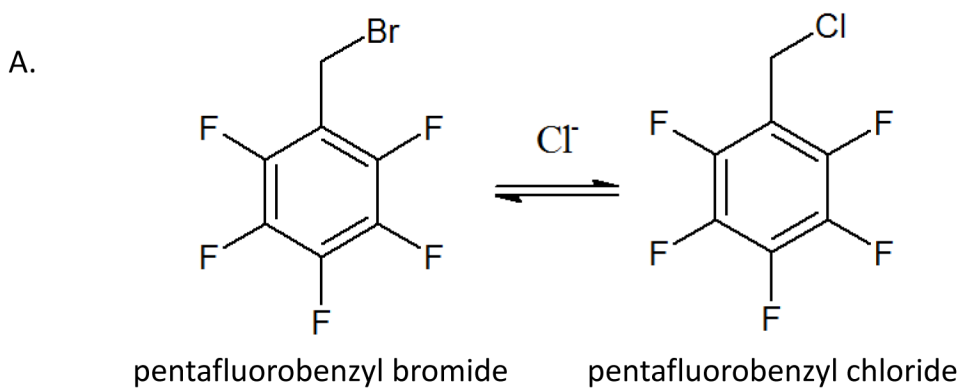


Figure 1.

A) Conversion of pentafluorobenzyl bromide to pentafluorobenzyl chloride. Although the reaction is reversible, the large excess of pentafluorobenzyl bromide pushes the equilibrium to the right. B) Representative chromatogram from a cytosolic liver fraction. *p*-hydroxybiphenyl elutes at 9 minutes, pentafluorobenzyl chloride elutes at 19.5 minutes, and the unreacted pentafluorobenzyl bromide elutes at 22 minutes.

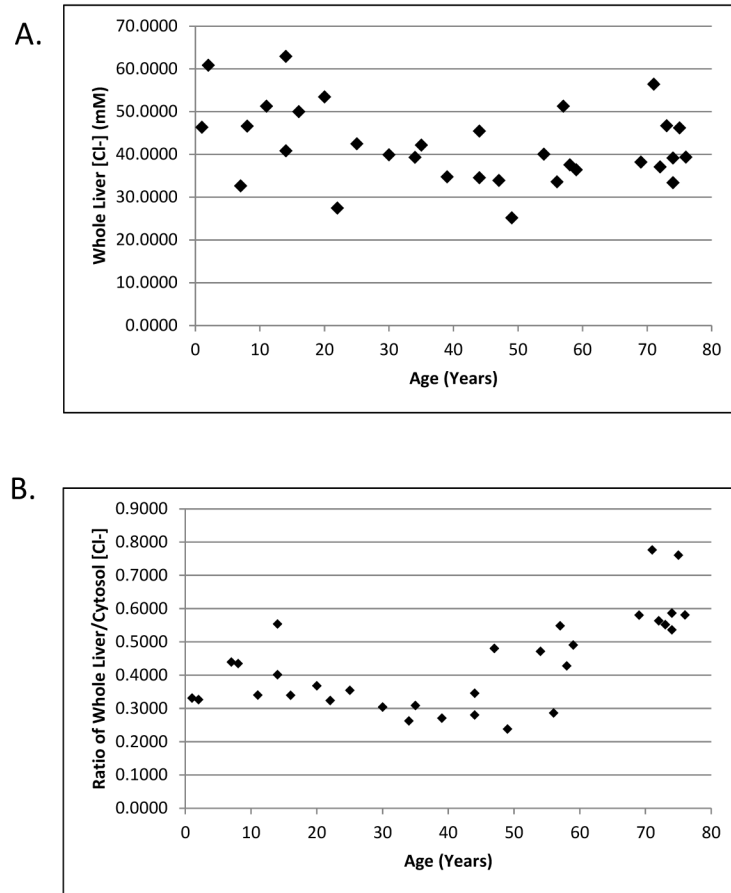


Figure 2. Chloride concentrations in whole liver homogenates. A) Measured chloride concentrations were plotted against donor age. B) The ratio of whole liver to cytosolic [Cl⁻] was plotted against donor age.

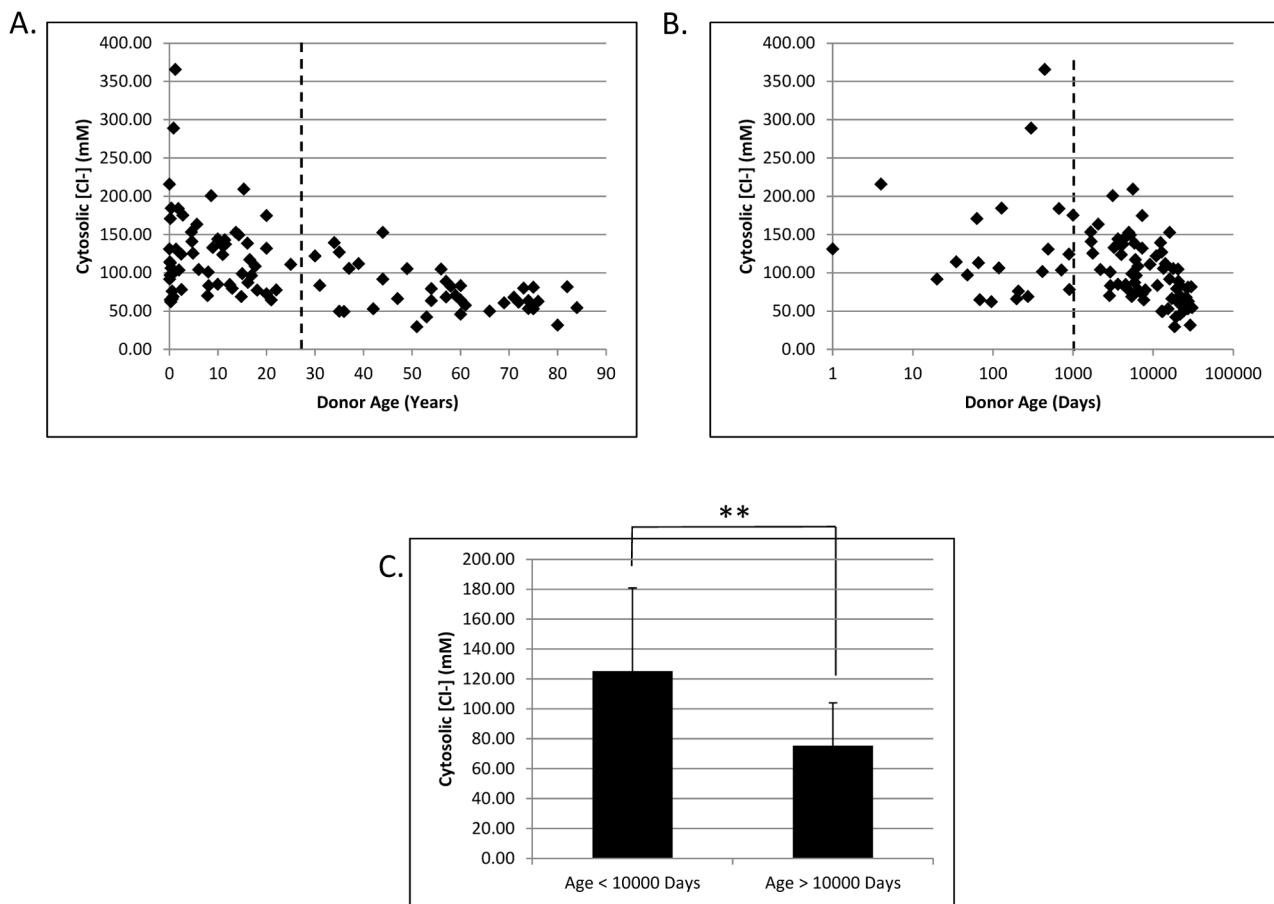


Figure 3. Changes in cytosolic liver chloride as a function of age. Calculated cytosolic chloride concentrations were plotted against donor age in years with a linear scale (A) and in days with a logarithmic scale (B). The dashed lines represent an arbitrary division between the high and low chloride samples at 10,000 days of age. Panel C shows a highly significant difference in cytosolic [Cl⁻] in livers from donors less than or greater than 10,000 days of age. ** denotes $p < 0.0001$ as determined by Student's T test.

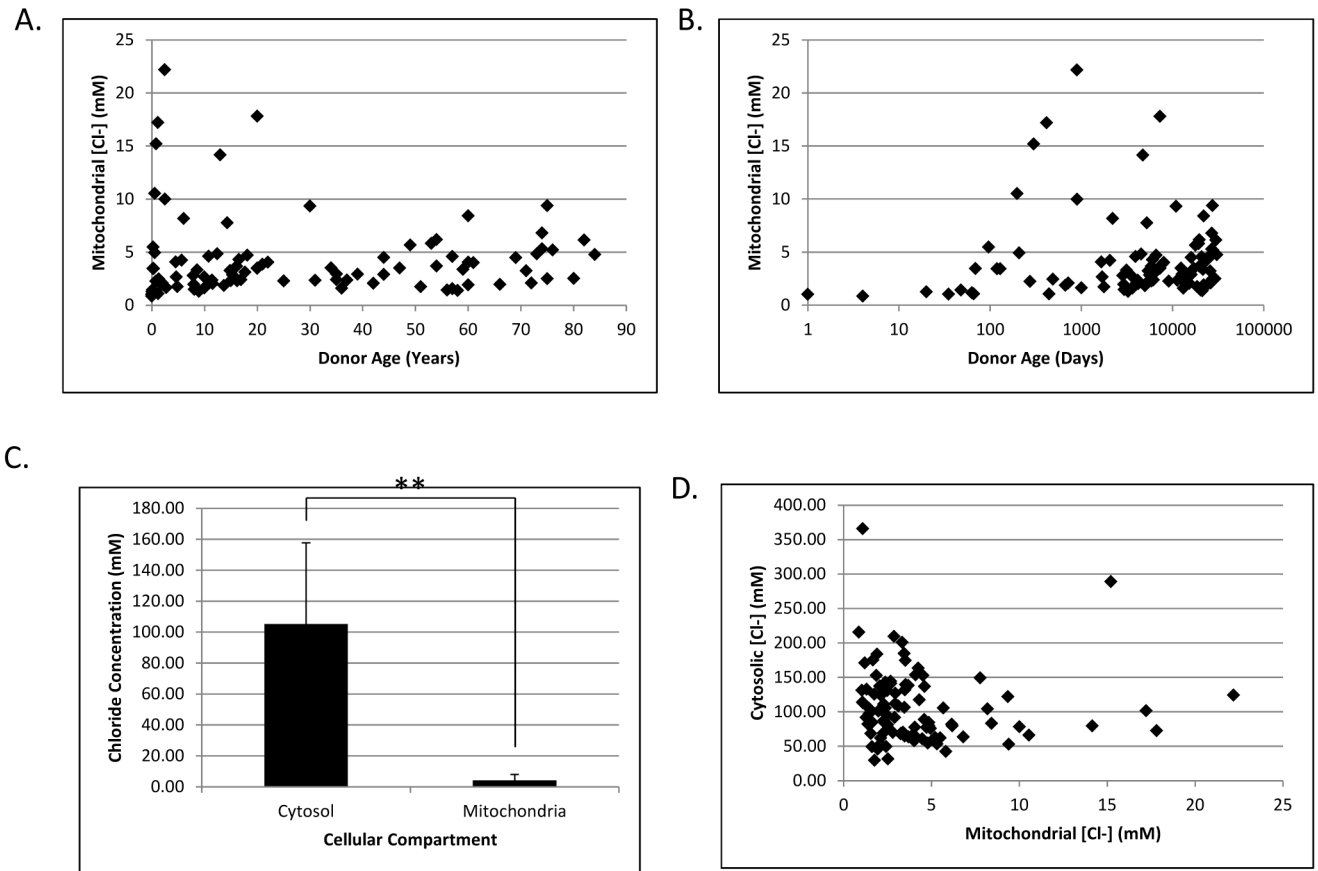


Figure 4.

Changes in mitochondrial chloride as a function of age. Calculated mitochondrial chloride concentrations were plotted against donor age in years with a linear scale (A) and in days with a logarithmic scale (B). C) Histogram showing the average $[Cl^-]$ in the cytosolic and mitochondrial compartments. Values represent the mean across all ages and error bars show the standard deviation. ** denotes $p < 0.0001$ as determined by Student's T test. D) Scatterplot showing the relationship between cytosolic and mitochondrial $[Cl^-]$ in individual donors.

Table 1

Chloride assay parameters. The number of replicates indicated were prepared for each standard curve. The curve from resuspension buffer was used for mitochondria, from phosphate buffer for cytosol and from water for the whole liver analyses.

Linear range, mM	Matrix	Slope	Intercept	R ² value
0.01 to 1 (n=3)	Resuspension buffer	0.131 ± 0.014	0.131 ± 0.006	0.976 ± 0.007
0.05 to 7.5 (n=3)	Phosphate buffer	0.138 ± 0.003	0.118 ± 0.018	0.993 ± 0.009
5 to 20 (n=2)	Water	0.150 ± 0.002	0.088 ± 0.039	0.997 ± 0.001